



IJRASET

International Journal For Research in
Applied Science and Engineering Technology



INTERNATIONAL JOURNAL FOR RESEARCH

IN APPLIED SCIENCE & ENGINEERING TECHNOLOGY

Volume: 11 **Issue:** X **Month of publication:** October 2023

DOI: <https://doi.org/10.22214/ijraset.2023.55946>

www.ijraset.com

Call:  08813907089

E-mail ID: ijraset@gmail.com

Quality and Feature Analysis of Parent and Child Fingerprints in West Bengal, India

Diptadip Maiti¹, Madhuchhanda Basak², Debashis Das³

Department of CSE, Techno India University, Saltlake, Kolkata, West Bengal, India-700091

Abstract: Fingerprint image of father, mother and child in ink paper method are collected from the region of West Bengal, India. One Hundred family without having kinship relation are involved in the data collection process. The paper is scanned with a HP scanner with 1200 ppi resolution and pre-processed with different technique to form a dataset of 1500 fingerprint images. Different non reference and reference image quality assessment technique are applied to test the quality of the image dataset. Minutiae based feature are extracted from the images to find a correlation between child and parent's fingerprints. This family fingerprint dataset can be used by the researchers to find an alternative of DNA matching for parental verification or other research works.

Keywords: Biometrics, Family Fingerprint Dataset, Paternity Test, Minutiae feature analysis, Fingerprint Quality Assessment.

I. INTRODUCTION

The biometric based authentication system become the post popular and useful form of personal identification. Moreover, fingerprint-based system provides most ease access and cost-effective solution in the market [1]. With the exception of mishaps, including cuts and bruises on the finger tips, a person's finger ridge configurations don't vary throughout the course of their lifespan. When the fetus has grown for around seven months, fingerprints are fully developed. Fingerprints are a component of an individual's phenotype, which results from the interplay of the individual's genes with the developmental environment in the uterus [2]. For years, people have been debating whether human fingerprints and other features are inheritable. Almost all characteristics in the offspring share genetic information from the parents, according to geneticists [3]. The size, shape, and spacing of the ridges and the inheritance of fingerprint patterns have been shown to be strongly correlated by early pioneers in the subject of dermatoglyphics (the study of friction ridge skin patterns). Fingerprints have a trait that is inherited. While some pattern types are frequently inherited genetically, finger-prints' individual characteristics are not [4]. There is a lack of scientific research on the fingerprint pattern resemblance in families using the qualitative attributes available in the dataset [5]. On the other hand, quality of the input data has an impact on biometric recognition systems, just as other applications of pattern recognition and machine learning. As a result, it's crucial to quantitatively assess a sample's quality in order to establish whether it can be used as a biometric or not. Lack of standards have inescapably resulted in the spread of results that are contradictory, incomparable, and non-replicable [7]. The uniformity and strength of the ridge patterns are assessed using methodologies for evaluating fingerprint quality [6]. The characteristics of the ridge patterns and the sample's performance at recognition are directly related [8] [9] [10].

During the study, samples from 100 families are collected to form a family fingerprint dataset for the researchers to test similarity between child and parent fingerprints. The collected fingerprints are analysed and checks for quality using non reference and reference methods. The manuscript is organized as follows: Section II, the importance of the dataset is described. Section III present the internal details of the dataset. Section IV describe the experimental setup. Section V represents the reference and non-reference image quality analysis with minutiae-based image feature analysis. Section VI draws the concluding remarks. Future directive of the present work is enlisted in Section VII.

II. IMPORTANCE OF DATASET

Demographically separated and good quality with standardized family fingerprints dataset may be in need of the research community for operational recognition and evaluation of different state of the art techniques in near future. The importance of the created dataset and the possible use are highlighted below:

- 1) Researchers may take hold of the dataset to check whether some relation can be established between parents and children's and may be used as an alternative of costly DNA matching.
- 2) Family fingerprints plays an important role in identification of victims of natural or man-made disasters such as tsunami, earth quake, flood, pandemic or war bombing. Victims body may be identified with the help of fingerprint where face recognition is not possible and other document are missing.

- 3) Applications for government employment, passport or other identity document verification and defense security clearness, family fingerprints may play an important role.
- 4) Identification of genetic deceases such as amnesia or other unknown decease family fingerprints may act as a dependable tool.
- 5) Banking and finance sector may use family fingerprints dataset to identify true patrimony in case of sudden or accidental death of a client.
- 6) Proper maintenance and continuous updating of family fingerprint dataset may be useful to track infants' vaccination and nutrition records.

III. DESCRIPTION OF DATASET

We involve 100 families from the West Bengal region in India to collect the fingerprint data. We have collected five fingerprints of five fingers of each person's right hand which comprises a total of 1500 images. The age range of parents is in between 20 years to 60 years and children age is between 5 years to 25 years. Table I represents the description of the Dataset.

TABLE I

Dataset Description	
Subject:	Computer Science
Domain:	Pattern Recognition, Biometric, Image Processing
Data type:	Image
Data format:	Gray Scale PNG image
Location:	West Bengal, India
Size:	1500 image
Sample:	100 families
Parameter:	Right hand five finger with parent age from 20-60 yr and child age from 5-25yr.
Description:	The data was collected from 100 families taking five fingerprint image from father, mother and child's right hand comprising 1500 total images.
Data Acquisition:	Direct from the individual.
Accessibility:	The data are available with this article.

IV. EXPERIMENTAL DESIGN AND METHODS

The fingerprints are initially collected with paper and ink methods. The paper is scanned with a hp scanner with 1200 ppi resolution. Subsequently the images are cropped with 512 x 512 size. Preprocessing like normalization, ridge orientation estimation, reliability estimation, ridge frequency calculation, region of interest detection and finally Gabor filtering methods are applied to get enhanced image. Figure 1 shows some sample of the father, mother and children's fingerprint of the same family. The details of different fingerprints are provided in Table II that are available in the dataset. The preprocessing step are shown in Figure 2.

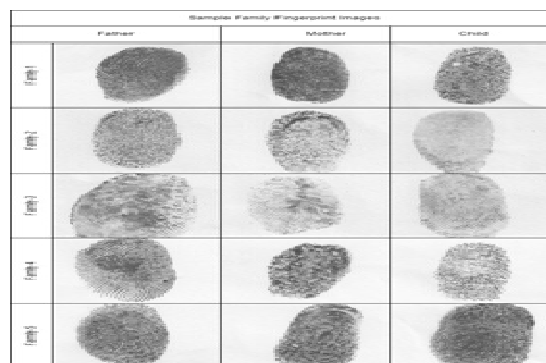


Fig. 1. Sample Fingerprint Image of the Dataset

TABLE II
Dataset Details

No	Fingerprint Type	Quantity
1	Father's Fingerprint	500 Fingerprints
2	Mother's Fingerprint	500 Fingerprints
3	Children's Fingerprint	500 Fingerprints

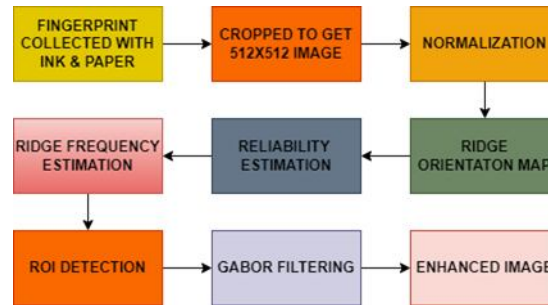


Fig. 2. Preprocessing of Fingerprint Image

V. DATASET ANALYSIS

A. Image Quality Analysis

In a comparative environment, quality score is a quantitative expression of the utility or predicted performance of a biometric sample. A number of approaches have been proposed in the literature for evaluating image quality in objective measure. Assessment of image quality can be categorized into two main categories.

- Quality Analysis without Reference Image
- Quality Analysis using Reference Image

An available reference image is a requirement and an essential component of full reference image quality assessment approaches. On the other hand, an image with a possible distortion is evaluated only on its own perceived quality in non-reference image quality assessment approaches. Figure 3 represents the list of image quality metrics that have been applied to check the quality of the dataset [11].

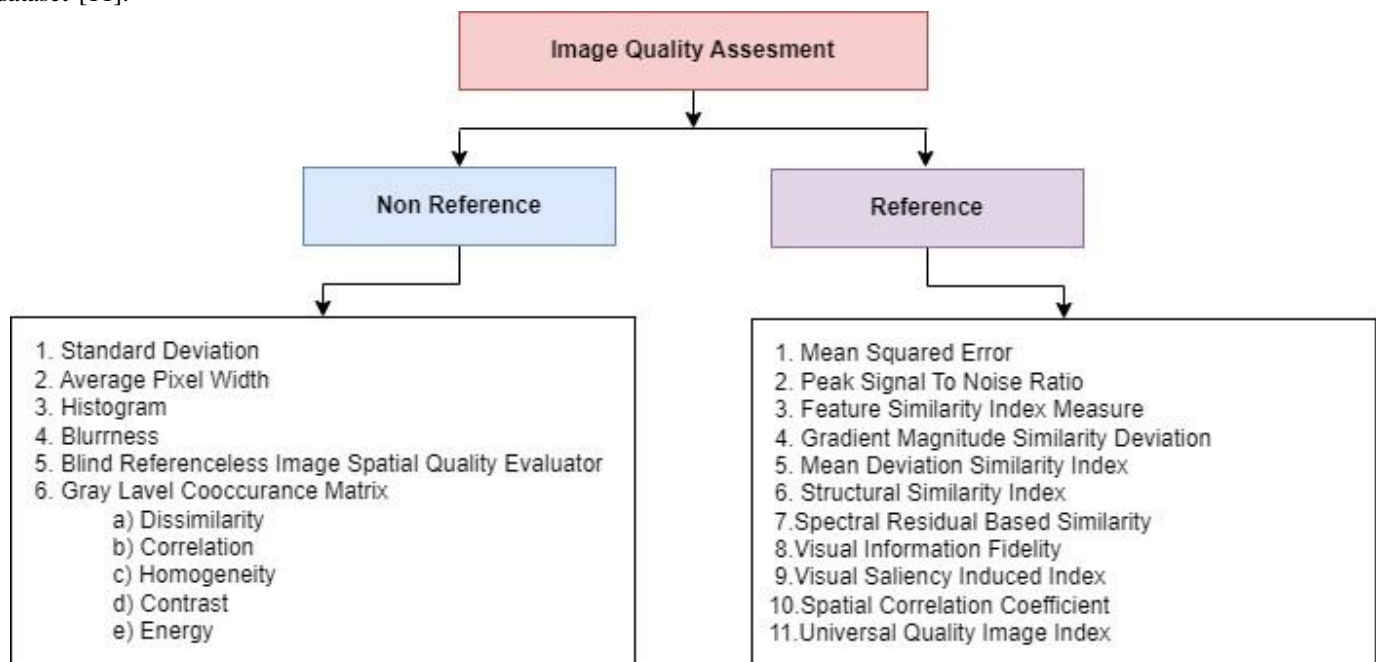


Fig. 3. Image Quality Metrics

1) *Non-Reference Image Quality Analysis*

Without using any perfect, reference images, no-reference image quality assessment (NR-IQA) aims to forecast how well an image will be received by verification system [12].

a) *Standard Deviation*

It measures how widely apart observations are from their means within a dataset. Sigma () stands for the square root of the variance. Standard deviation measures how much the data set’s observations deviate from its mean because it is expressed in the same unit as the dataset’s values. Mathematically:

$$\sigma = \sqrt{\frac{\sum_{i=1}^m \sum_{j=1}^N [\text{img}(i, j) - \bar{m}]^2}{M \times N}} \tag{1}$$

where $\text{img}(i, j)$ represents the pixel value at position (i, j) of an image of size $M \times N$ signifies the mean value of all pixel. This is the best measure for evaluating the quality of recovered pictures, and it may be utilized in situations where the image has been deteriorated owing to distributions such as Gaussian and impulsive noises. Fig 4 shows the plotting of standard deviation value of the dataset.

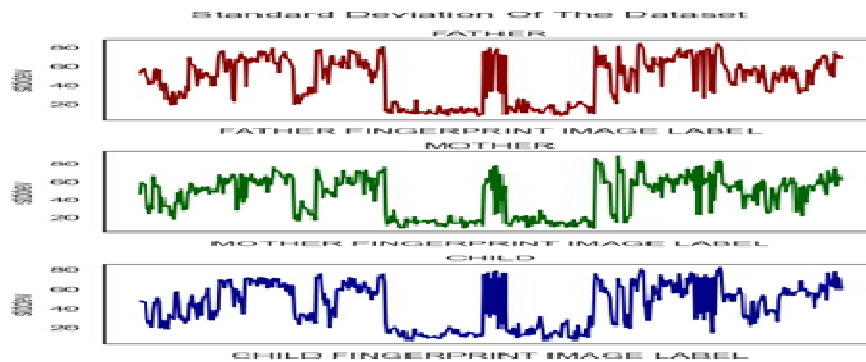


Fig. 4. Plotting of Standard Deviation of Dataset

b) *Average Pixel Width*

Some images could be completely uniform and devoid of any pixel fluctuation. Average Pixel Width is a metric that shows how many edges are in an image. If this value turns out to be extremely low, the image is probably uniform and may not accurately depict the content.

$$apw = \frac{\text{edge}_{count}}{\text{img}_{height} * \text{img}_{width}} \tag{2}$$

c) *Blurriness*

In this method, the Laplacian filter is convolved with the single channel of an image. The blurriness of the image depends on whether the supplied value is smaller than a threshold value or not.

$$\begin{bmatrix} 0 & 1 & 0 \\ 1 & -4 & 1 \\ 0 & 1 & 0 \end{bmatrix} \tag{3}$$

Figure 5 shows the plotting of average pixel width and blurriness of the father, mother and child images of the dataset.

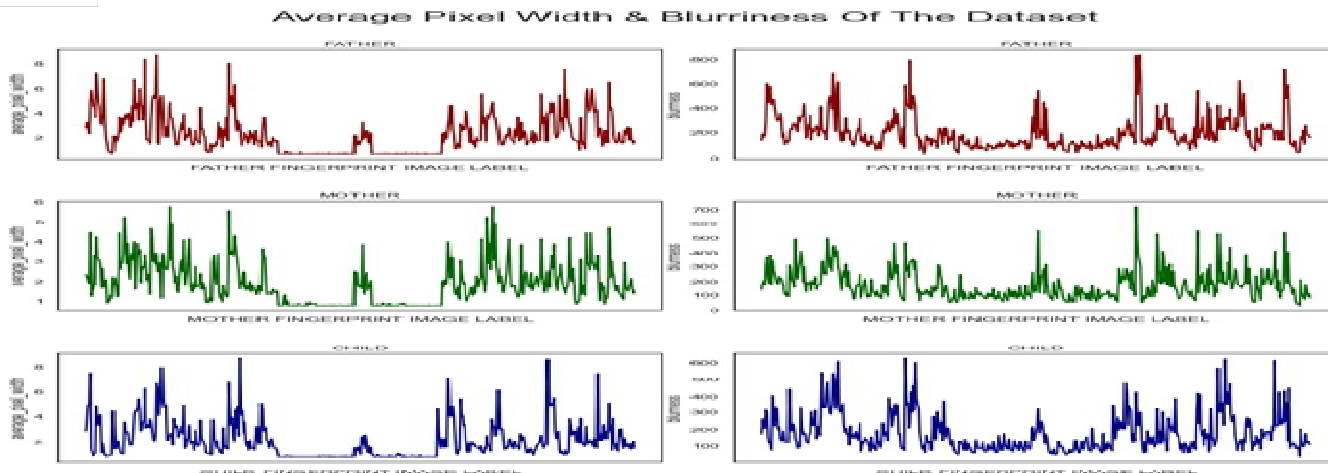


Fig. 5. Average Pixel Width & Blurriness of Dataset

d) Histogram

A histogram is a graphical depiction of data points arranged into ranges that is user specifies. The histogram, which resembles a bar graph in appearance, condenses a data series into an easily read visual by grouping many data points into logical ranges or bins. By looking at the histogram for a specific image a viewer will be able to judge the entire tonal distribution at a glance. It is used to analyze an image. Properties of an image can be predicted by the detailed study of the histogram and brightness of the image can be adjusted by having the details of its histogram. Figure 6 shows histogram of one fingerprint of father, mother and child of the dataset.

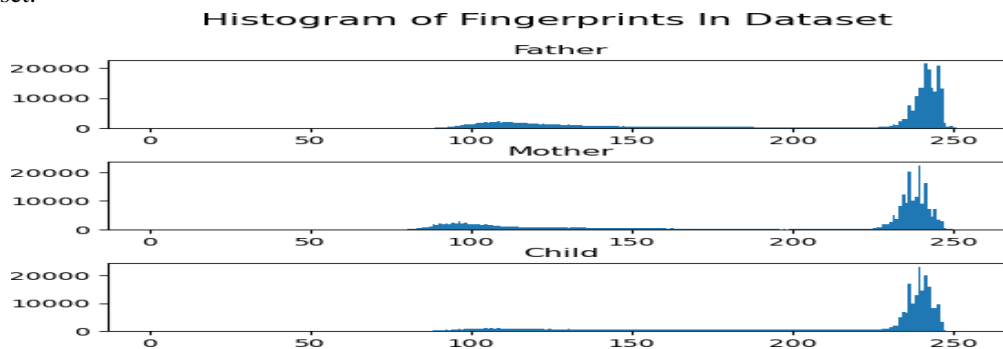


Fig. 6. Histogram of Single Fingerprints of a Family

e) Brisque

Unreferenced and Blind Image Spatial Quality Evaluator (BRISQUE) assesses the degree of image naturalness (or lack thereof) based on measurable departures from a natural image model and extracts the point-wise statistics of local normalized luminance signals [13]. It does not calculate distortion-specific characteristics like ringing, blur, or blocking, but rather employs scene statistics of regionally normalized brightness coefficients to quantify probable picture losses owing to the presence of distortions, resulting in a holistic assessment of quality.

$$img(i, j) = \frac{img(i, j) - \mu(i, j)}{\sigma(i, j) + C} \tag{4}$$

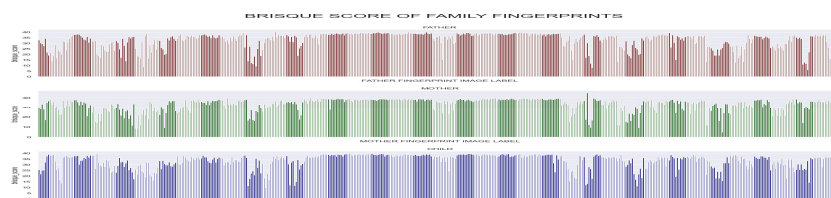


Fig. 7. BRISQUE Score of Family Fingerprints

where C is a constant. If $img(i, j)$ domain is $[0, 255]$ then $C=1$ if the domain is $[0, 1]$ then $C=1/255$. The BRISQUE score from an image will be a positive value range from 0 to 100. A low BRISQUE measure indicates that the image is having high quality. Figure 7 plots the brisque score of father, mother and child fingerprint.

f) *Grey Level Co-occurrence Matrices (GLCM)*

One of the crucial factors in detecting items or areas of interest in an image is texture. A co-occurrence distribution, also known as a co-occurrence matrix, is one of several terms for it. Distribution, which is defined over an image, is the distribution of values that occur at a given offset represents the distance and angular spatial relationship across a specified region of a specific size within an imaging direction of Analysis are $0^0, 45^0, 90^0$ and 135^0 [14]. The second order statistical feature extracted by the GLCM may be used for achieving high discrimination accuracy which requires less computation time and hence may be efficiently used for real time Pattern recognition applications. It characterizes the texture of an image by calculating how often pairs of pixels with specific values and in a specified spatial relationship occur in an image.

- *Contrast*

Returns a metric for the overall intensity contrast between a pixel and its neighbors. For a constant picture, contrast is 0. The building Variation and inertia are other names for contrast.

$$contrast = \sum_{i,j} img(i, j)^2 \tag{5}$$

- *Correlation*

Reveals a pixel's correlation with its neighbors over the entire image. For an image that is perfectly positively or negatively correlated, correlation is either 1 or -1.

$$correlation = \sum_{i,j} \frac{img(i, j)}{1 + |i - j|} \tag{6}$$

- *Energy*

Gives the GLCM's squared elements' sum. Energy for a steady picture is 1. The building the terms uniformity, uniformity of energy, and angular second moment are also used to refer to energy.

$$Energy = \sum_i \sum_j \{img(i, j)\}^2 \tag{7}$$

- *Homogeneity*

Returns a value that represents how closely the GLCM diagonal is matched by the distribution of its elements. For adiaagonal GLCM, homogeneity is 1.

$$Homogeneity = \sum_{i=0}^{255} \sum_{j=0}^{255} \frac{img(i, j)}{1 + (i - j)^2} \tag{8}$$

- *Dissimilarity:*

Distance between pairs of objects (pixels) in the region of interest is measured by dissimilarity.

$$Dissimilarity = \sum_i \sum_j |i - j|img(i, j) \tag{9}$$

$$Dissimilarity = \sum_i \sum_j |i - j|img(i, j) \tag{9}$$

Table III represents sample GLCM values of single fingerprints of three families of the dataset.

TABLE III
GLCM VALUES OF FINGERPRINTS OF THREE FAMILY

Family	Member	Dissimilarity	Correlation	Homogeneity	Contrast	Energy
Family-1	Father	20.1168	0.3180	0.0571	710.945	0.0192
	Mother	22.5407	0.5192	0.0606	915.833	0.0165
	Child	29.2050	0.4765	0.0476	1444.657	0.0149
Family-2	Father	33.5563	0.0020	0.0273	1686.568	0.0133
	Mother	12.2006	0.2554	0.0828	244.467	0.0253
	Child	8.1115	0.3762	0.1261	112.420	0.0332
Family-3	Father	31.9061	0.2575	0.0338	1586.185	0.0123
	Mother	27.4956	0.3732	0.0472	1329.831	0.0173
	Child	31.2379	0.1286	0.0337	1523.496	0.0128

2) Reference Image Quality Analysis

In this method, the target image quality is measured with reference to a distortion free original image. We have used a sample good quality image shown in Figure 8 from the dataset to check the full reference image quality metric. A few of such quality assessment metrics are discussed below:



Fig. 8. Reference Image for Quality Check

a) Mean Squared Error (MSE)

The MSE is a measurement of the squared cumulative error between the original and noisy image. The lower value of MSE signifies better quality of the target image.

$$mse = \frac{\sum_0^{M-1} \sum_0^{N-1} [img_1(m, n) - img_2(m, n)]^2}{M * N} \tag{10}$$

where img_1 is the reference image, img_2 is the target image and M, N is the length and breadth of the two images in pixel. A higher value of MSE designates a greater difference amid the original image and processed image.

b) Peak Signal to Noise Ratio (PSNR)

PSNR is the ratio of an image’s greatest achievable power to the power of corrupting noise that influences the representation’s quality. To calculate the PSNR of a picture, it must be compared to an ideal clean image with the highest potential power. The higher the PSNR, the better the quality of the target image.

$$psnr = 10 \log_{10} \left(\frac{(l - 1)^2}{mse} \right) \tag{11}$$

where l is maximum possible intensity levels. Figure 9 shows the MSE & PSNR value of the dataset.

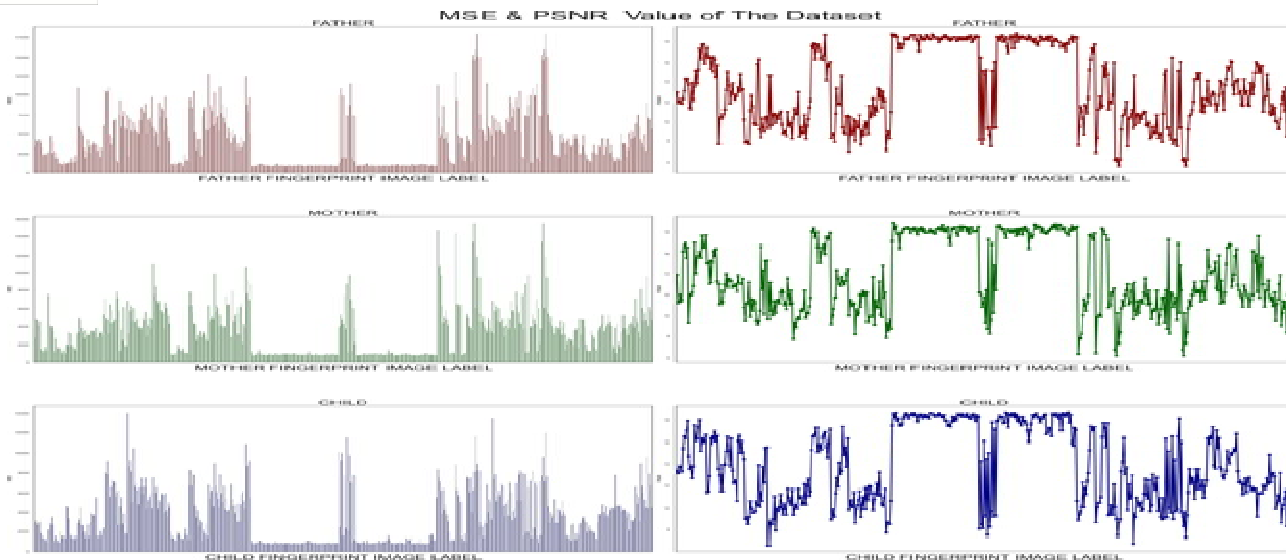


Fig. 9. MSE & PSNR Value of Dataset

c) *Feature Similarity Index (FSIM)*

Phase congruency (PC) and gradient magnitude in the Feature Similarity Index Measure serve complementary roles in describing the local quality of the image. Use phase congruency once more as a weighting function after obtaining the local quality map to arrive at a single quality score [15].

$$FSIM = \frac{\sum_{x \in \Omega} S_L(x) \cdot PC_m(x)}{\sum_{x \in \Omega} PC_m(x)} \quad (12)$$

where $S_L(\mathbf{x})$ is similarity at each location x , $PC_m(\mathbf{x})$ is the overall similarity between two image and Ω is the whole image spatial domain. The SSIM value is between 1 and -1 with 1 indicating perfect structural similarity.

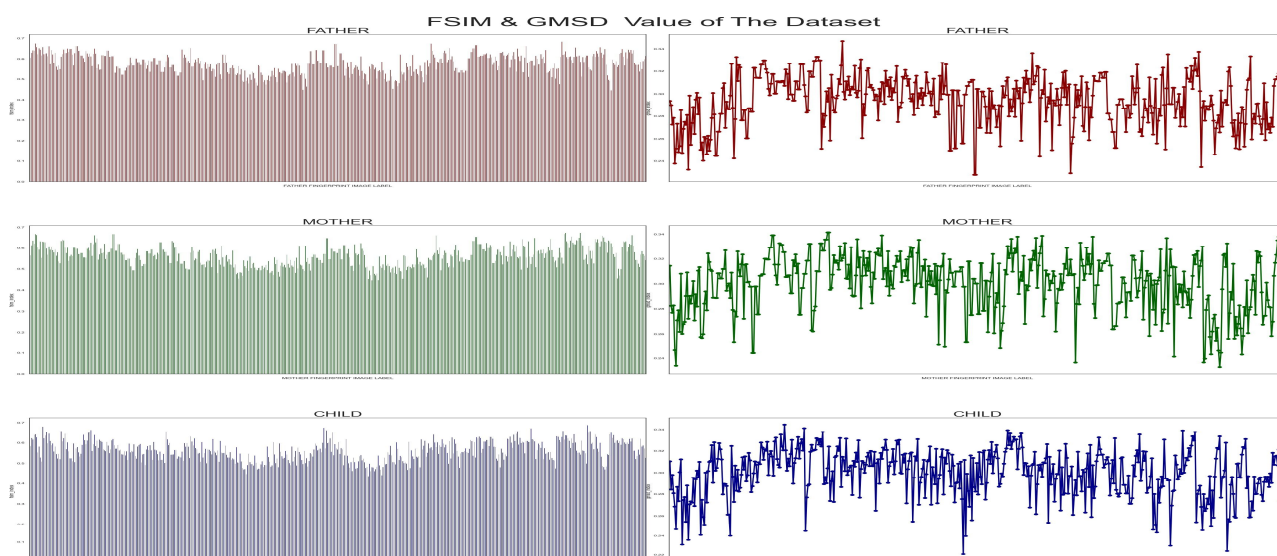


Fig. 10. FSIM & GMSD Value of Dataset

d) *Gradient Magnitude Similarity Deviation (GMSD)*

The local quality map of the distorted picture is calculated as the pixel-level similarity between the gradient magnitude maps of the reference and deformed images. The gradient magnitude similarity caused local quality map's standard deviation to forecast the final image quality rating [16].

$$gmsm = \frac{1}{x} \sum_{i=1}^x gms(i)$$

$$gmsd = \sqrt{\frac{1}{x} \sum_{i=1}^x (gms(i) - gmsm)^2}$$
(13)

where gms(i) is the gradient magnitude similarity map computed between reference and target image, gmsm is the Gradient Magnitude Similarity Mean, x is the number of pixels. Higher the GMSD value better the quality of the image. Figure 10 represents the FSIM & GMSD value of the dataset.

e) Mean Deviation Similarity Index (MDSI)

The method measures perceptual picture quality assessment using gradient similarity (GS), chromaticity similarity (CS), and deviation pooling (DP) [17].

$$MDSI = \left[\frac{1}{N} \sum_{i=1}^N \left| \widehat{GCS}_i^{1/4} - \left(\frac{1}{N} \sum_{i=1}^N \widehat{GCS}_i^{1/4} \right) \right| \right]^{1/4}$$

$$\widehat{GCS}(x) = \alpha GS(x) + (1 - \alpha) \widehat{CS}(x)$$
(14)

where \widehat{GCS} is the combined gradient similarity map & joint color similarity map and N is the number of pixel. Higher the MDSI value greater the image quality.

f) Structural Similarity Index (SSIM)

The brightness, contrast, and structure comparison measurements between the samples of the reference and test images constitute the basis of the SSIM formula [11].

$$SSIM(x, y) = \frac{(2\mu_x\mu_y + c_1)(2\sigma_{xy} + c_2)}{(\mu_x^2 + \mu_y^2 + c_1)(\sigma_x^2 + \sigma_y^2 + c_2)}$$
(15)

where μ_x is pixel sample mean of x, μ_y is pixel sample mean of y, σ_x^2 is variance of x, σ_y^2 is variance of y, σ_{xy} is covariance of x and y. $c_1 = (k_1L)^2$, $c_2 = (k_2L)^2$ are two variables to stabilize the division with weak denominator is dynamic range of the pixel-values. $k_1 = 0.01$ and $k_2 = 0.03$ by default. The SSIM value range from 1 to 1 and more the value close to 1 better the image quality. Figure 15 shows the MDSI and SSIM value of the dataset.

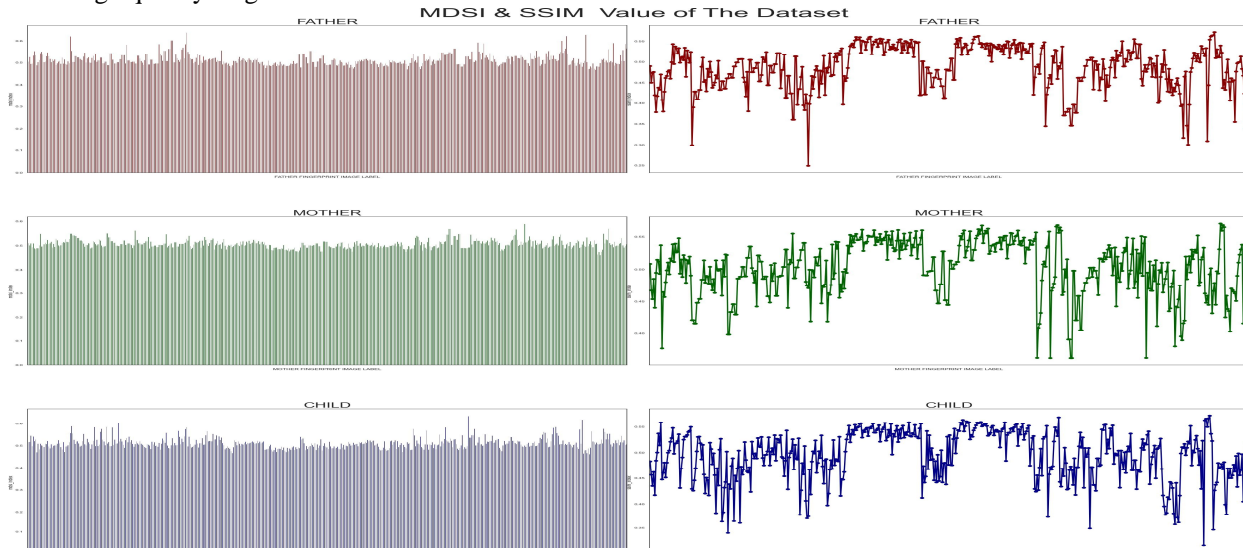


Fig. 11. MDSI & SSIM Value of Dataset

g) *Spectral Residual Based Similarity (SRSIM)*

SRSIM is based on the spectral residual visual saliency (SRVS), a powerful and practical visual saliency model. In SR- SIM, the SRVS map serves as both a feature map that describes the local quality of the image and a weighting function that denotes the significance of a local region [18].

$$SRSIM = \frac{\sum_{\mathbf{I} \in \Omega} S(\mathbf{I}) \cdot R_m(\mathbf{I})}{\sum_{\mathbf{I} \in \Omega} R_m(\mathbf{I})} \tag{16}$$

where $S(\mathbf{I})$ is local similarity, $R_m(\mathbf{I})$ overall similarity and Ω is whole image spatial domain. Lower the SRSIM value better is the image quality.

h) *Visual Information Fidelity (VIF)*

In VIF, an image information measure is used to determine how much of the reference image’s information can be retrieved from the distorted image [19].

$$VIF = \frac{\sum_{j \in \text{subbands}} I_1(\vec{C}^{N,j}; \vec{F}^{N,j} | s^{N,j})}{\sum_{j \in \text{subbands}} I_2(\vec{C}^{N,j}; \vec{E}^{N,j} | s^{N,j})} \tag{17}$$

$I_1(\vec{C}^{N,j}; \vec{F}^{N,j} | s^{N,j})$ and $I_2(\vec{C}^{N,j}; \vec{E}^{N,j} | s^{N,j})$ represent the information that can ideally be extracted from a particular channel in the reference and the test image respectively. Lower the VIF value better the target image quality. Figure 12 represents SRSIM & VIF value of the dataset.

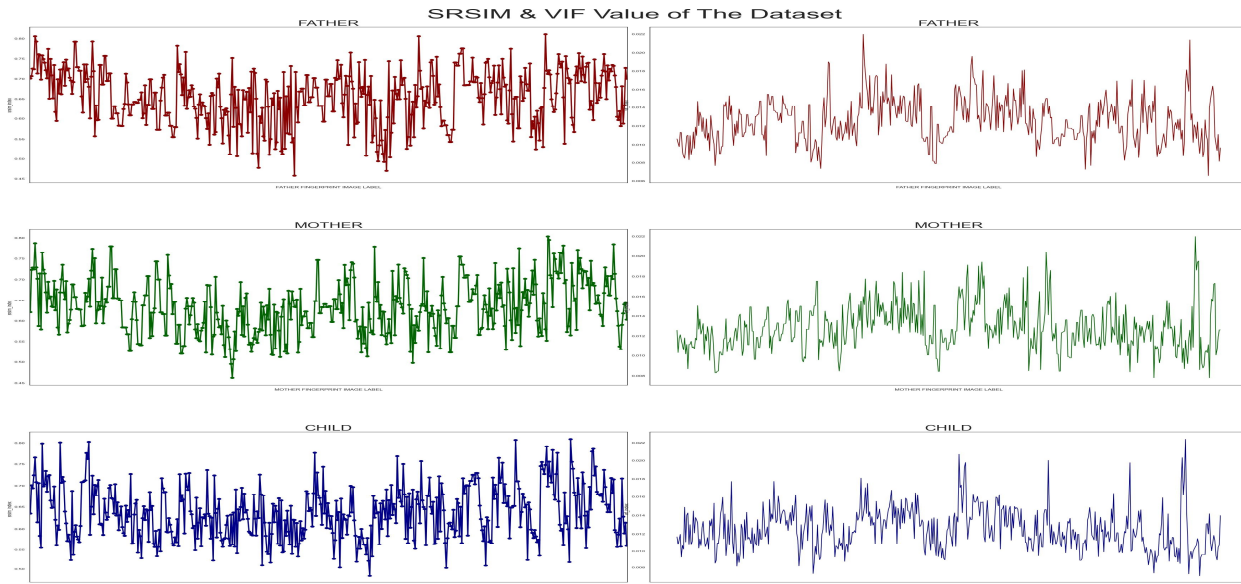


Fig. 12. SRSIM & VIF Value of Dataset

i) *Visual Saliency-Induced Index (VSI)*

When calculating the local quality map of the warped image, visual saliency (VS) is taken into consideration as a feature. Second, VS is used as a weighting function when pooling the quality score to account for the significance of a local area [20].

$$VSI = \frac{\sum_{\mathbf{I} \in \Omega} S(\mathbf{I}) \cdot VS_m(\mathbf{I})}{\sum_{\mathbf{I} \in \Omega} VS_m(\mathbf{I})} \tag{18}$$

where $S(\mathbf{I})$ is similarity measure, $VS_m(\mathbf{I})$ is visual saliency and Ω is whole image spatial domain. Higher the VSI value better the image quality.

j) *Spatial Correlation Coefficient (SCC)*

To combine the TM reflective bands with SPOT PAN and compare spectrally and spatially, use a wavelet multiresolution decomposition approach [21].

$$SCC = \frac{1}{n} \sum_i \sum_j |I'_{kij} - I_{kij}| \tag{19}$$

where I'_{kij} and I_{kij} are the pixel values of reference and original thematic mapper images, respectively. k is the k th band and i, j are the i th row and the j th column, respectively. Lower the SCC value better the image quality. Figure 13 shows the plotting of VSI & SCC values of the entire dataset.



Fig. 13. VSI & SCC Value of Dataset.

k) *Universal Quality Image Index (UQI)*

Loss of correlation, luminance distortion, and contrast distortion are the three elements that are combined to simulate any picture distortion in Index [22].

$$UQI = \frac{4\sigma_{pq}\bar{p}\bar{q}}{(\sigma_p^2 + \sigma_q^2)[(\bar{p})^2 + (\bar{q})^2]} \tag{20}$$

where p and q are reference, target image respectively and σ_p and σ_q are estimate of contrast of p and q respectively which can be calculated by the following:

$$\begin{aligned} \bar{p} &= \frac{1}{N} \sum_{i=1}^N p_i, & \bar{q} &= \frac{1}{N} \sum_{i=1}^N q_i \\ \sigma_p^2 &= \frac{1}{N-1} \sum_{i=1}^N (p_i - \bar{p})^2, & \sigma_q^2 &= \frac{1}{N-1} \sum_{i=1}^N (q_i - \bar{q})^2 \\ \sigma_{pq} &= \frac{1}{N-1} \sum_{i=1}^N (p_i - \bar{p})(q_i - \bar{q}) \end{aligned}$$

Higher the UQI value better the image quality. Figure 14 represents plotting of the UQI values obtained from the dataset.

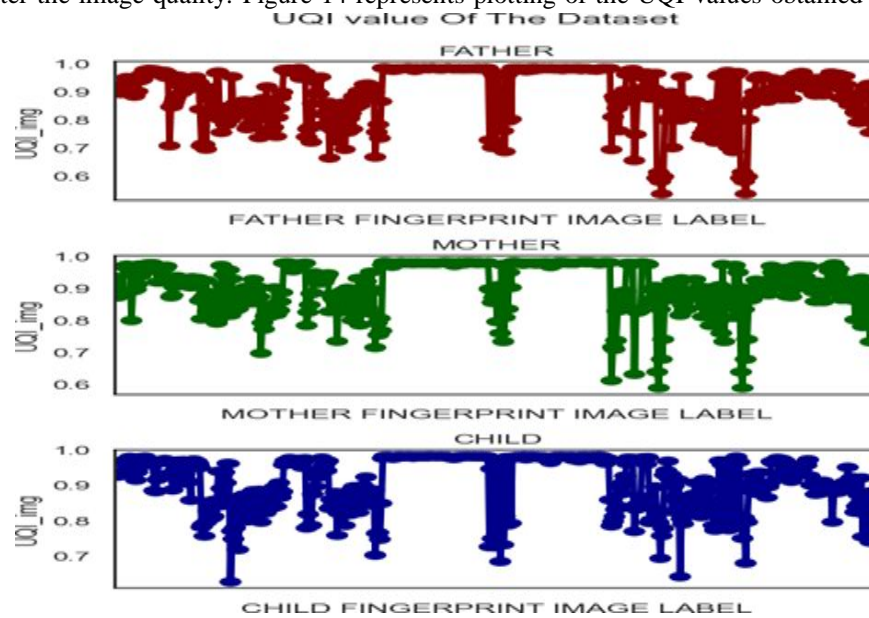


Fig. 14. Universal Quality Image Index Value of Dataset.

B. Image Feature Analysis

Extraction of minutiae, ridge ends and bifurcation points, allows for fine-level fingerprint comparison. Five categories —arch, tented arch, left loop, right loop, and whorl are used to categories fingerprints [23]. Figure 15 shows the minutiae detected fingerprint images considered randomly from three different families of the dataset. The red circles depict the ridge ending points whereas the green squares are representing the bifurcations [26].

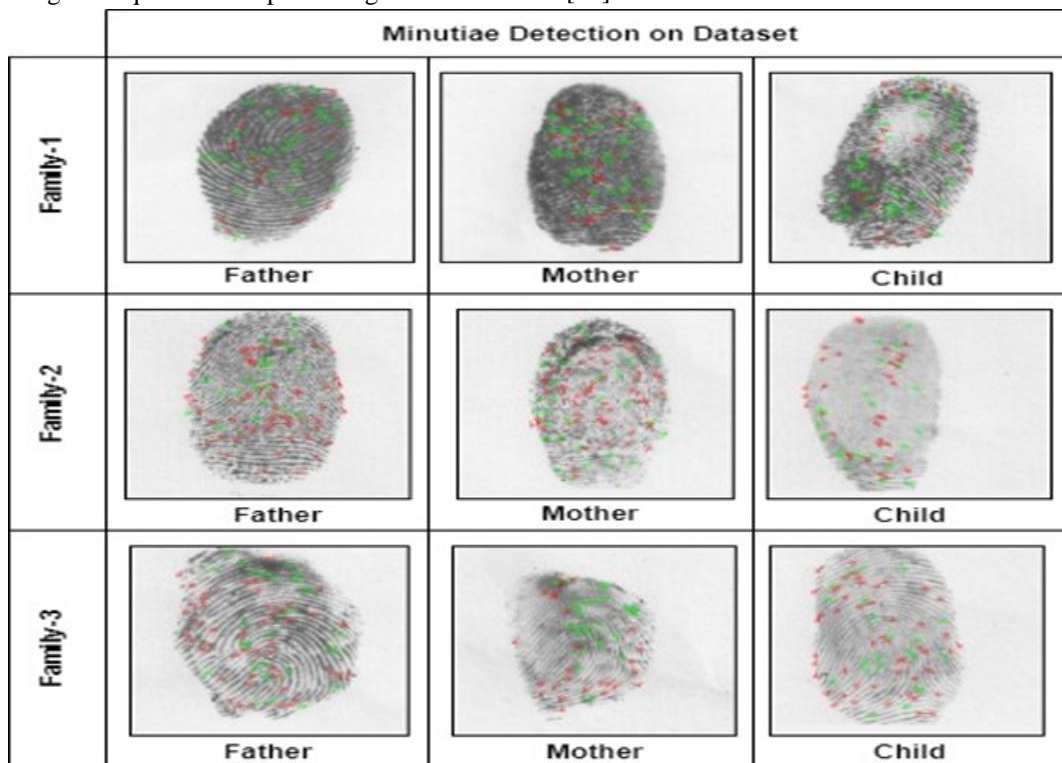


Fig. 15. Minutiae Detected Family Fingerprint

Figure 17 shows the plotting of different categories of fingerprints of father, mother and child fingerprints available in the entire dataset.

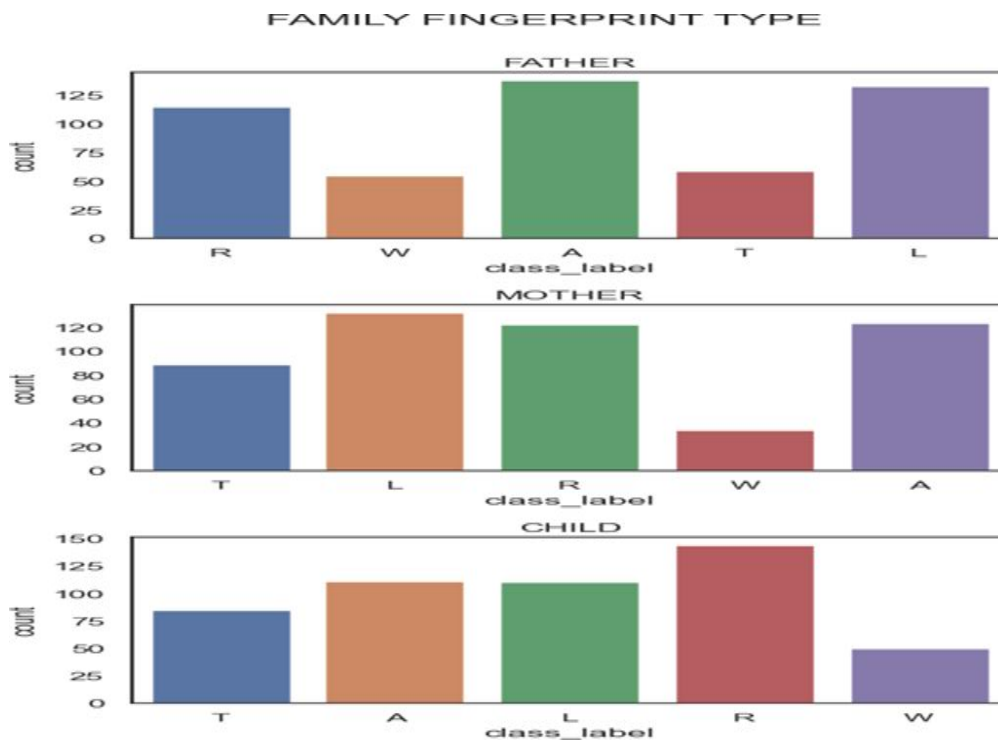


Fig. 16. Category of Fingerprints Available in Dataset

The minutiae points can be classified into six classes viz. ending, bifurcation, fragment, enclosure, crossbar and others [24][25]. Table IV shows a few samples of such different classes that have been detected from the family fingerprint dataset. Overall analysis of the dataset using different image quality assessment technique suggested that 65% image in the dataset are good quality and remaining 35% are challenging in nature.

TABLE IV
Sample Minutiae Classes Detected From Single Fingerprint Of The Dataset

Family	Member	Minutiae No	Ending No	Bifurcation No	Fragment No	Enclosure No	Crossbar No	Other No
Family-1	Father	54	17	2	0	9	15	11
	Mother	33	9	0	0	3	4	17
	Child	21	6	0	0	6	6	3
Family-2	Father	37	4	2	0	9	4	18
	Mother	13	6	0	0	0	3	4
	Child	48	8	1	0	13	10	16
Family-3	Father	26	5	0	0	10	3	8
	Mother	29	12	1	0	6	1	9
	Child	48	22	2	0	4	7	13
Family-4	Father	44	10	2	0	10	9	13
	Mother	57	13	2	0	13	15	14
	Child	41	11	0	0	14	7	9
Family-5	Father	55	10	1	0	12	4	28
	Mother	32	16	0	0	3	4	9
	Child	22	7	0	0	3	7	5

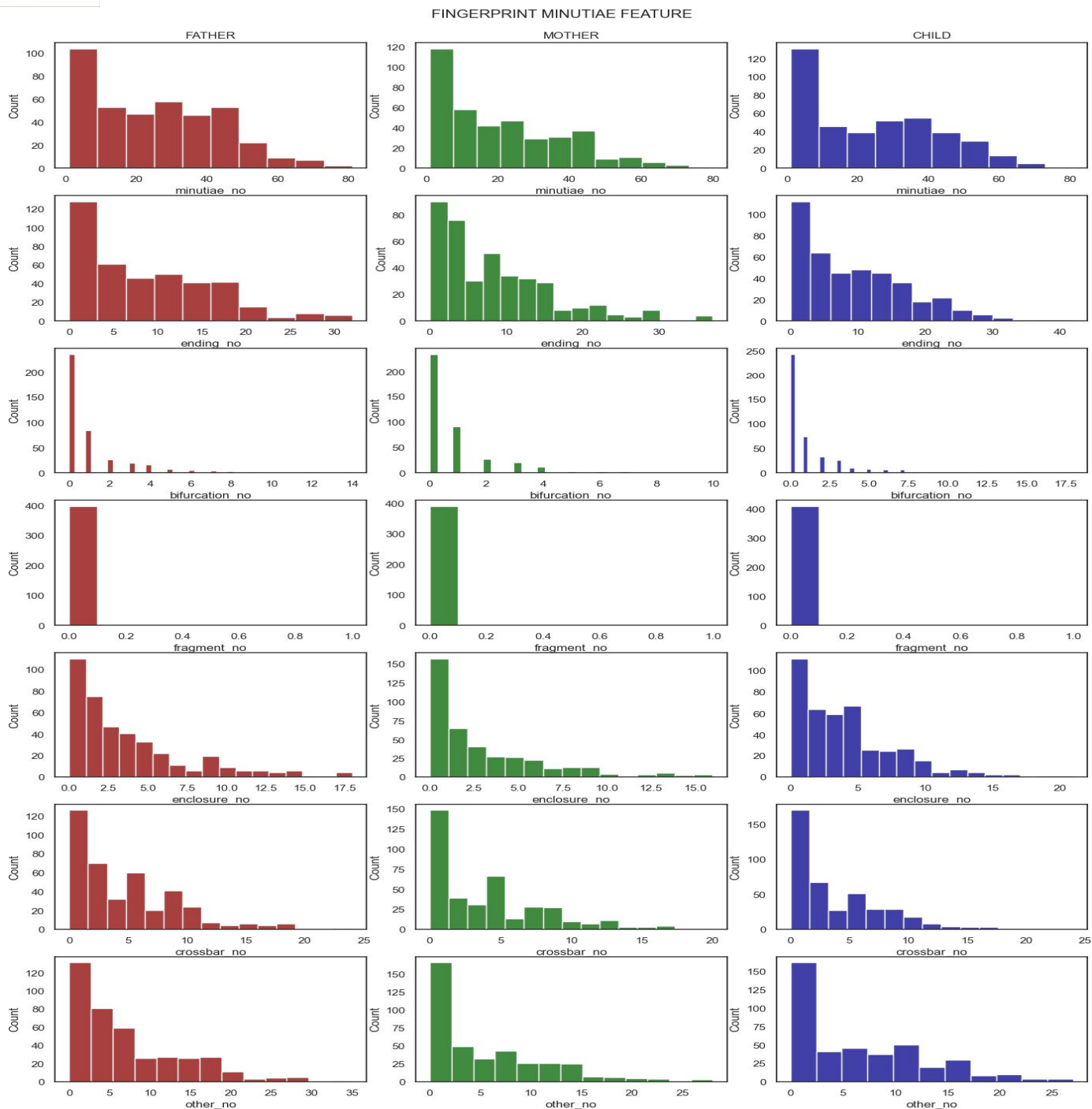


Fig. 17. Minutiae Analysis of The Whole Dataset

VI. CONCLUSION

This paper makes an effort to investigate the existence of genetic relationships among family members utilizing minute traits. The fingerprints are collected from father, mother, and child of same families. To create the improved image, pre- and post-processing are applied to the fingerprint images. Additionally, it has been noted that the majority of family members have comparable ridge patterns. The assertion that fingerprints carry hereditary relationships is made easier by the premise that fingerprint patterns are genetically determined. Given that they share 50% of the same genes, fingerprint patterns of parents and children exhibit some universal similarities. To authenticate the fingerprints for clinical studies, similar discoveries may also be explored with a varied set of family spreads in a large population area.

VII. FUTURE SCOPE

A more research is required on the examination of the genetic relationships and inherited pattern conditions based on family fingerprints, more research is required. A more effective evaluation methodology is required for biometric quality assessment metrics. Statistical tests and a strong association with match score performance can help with more accurate evaluation. Researchers must place a considerable emphasis on computation cost while designing quality evaluation approaches, which must be less than or equal to the matching time. The sensor that is being used to collect the fingerprint sample greatly determines its quality. The majority of quality measures should evaluate ridge clarity and the number of detected minutia because auto capture is a popular function in contemporary fingerprint sensors, necessitating real-time quality assessment of the given sample. Infants of age less than 5 years may be included in dataset collection which may reveal broad scope of research.

REFERENCES

- [1] Y. Han, C. Ryu, J. Moon, H. Kim and H. Choi, "A Study on Evaluating the Uniqueness of Fingerprints Using Statistical Analysis," in Information Security and Cryptology – ICISC 2004, vol. 3506, p. 467–477.
- [2] E. O. AIGBOGUN, C. P. Ibeachu and A. M. Lemuel, "Fingerprint pattern similarity: a family-based study using novel classification," *Anatomy*, vol. 13, p. 107–115, August 2019.
- [3] D. Asen, "Fingerprints and paternity testing: a study of genetics and probability in pre-DNA forensic science," *Law, Probability and Risk*, vol. 18, p. 177–199, September 2019.
- [4] S. E. Obaje, "Hereditary trends in parent and offspring fingerprint classes," in 2011 3rd International Conference on Electronics Computer Technology, Kanyakumari, 2011.
- [5] S. Yoon and A. K. Jain, "Longitudinal study of fingerprint recognition," *Proc. Natl. Acad. Sci. U.S.A.*, vol. 112, p. 8555–8560, July 2015.
- [6] K. Chockaian, R. Vayanaperumal and B. R. Kanagaraj, "New approach for identifying hereditary relation using primary fingerprint patterns," *IET Image Processing*, vol. 7, p. 423–431, July 2013.
- [7] F. Alonso-Fernandez, J. Fierrez and J. Ortega-Garcia, "Quality Measures in Biometric Systems," p. 11, 2012.
- [8] C. Karthikeyini, V. Rajamani and K. B. Raja, "Exploring fingerprints using composite minutiae descriptors to determine hereditary relation across multiple generations," *IJBET*, vol. 15, p. 224, 2014.
- [9] S. Bharadwaj, M. Vatsa and R. Singh, "Biometric quality: a review of fingerprint, iris, and face," *J Image Video Proc*, vol. 2014, p. 34, December 2014.
- [10] Z. Yao, J.-M. L. Bars, C. Charrier and C. Rosenberger, "Fingerprint Quality Assessment: Matching Performance and Image Quality," in *Biometric Security and Privacy*, R. Jiang, S. Al-maadeed, A. Bouridane, P. D. Crookes and A. Beghdadi, Eds., Cham, Springer International Publishing, 2017, p. 1–19.
- [11] Z. Wang, A. C. Bovik, H. R. Sheikh and E. P. Simoncelli, "Image Quality Assessment: From Error Visibility to Structural Similarity," *IEEE Trans. on Image Process.*, vol. 13, p. 600–612, April 2004.
- [12] J. C. Wu and C. L. Wilson, "Nonparametric analysis of fingerprint data on large data sets," *Pattern Recognition*, vol. 40, p. 2574–2584, September 2007.
- [13] A. Mittal, A. K. Moorthy and A. C. Bovik, "Blind/Referenceless Image Spatial Quality Evaluator," in 2011 Conference Record of the Forty Fifth Asilomar Conference on Signals, Systems and Computers (ASILOMAR), Pacific Grove, CA, USA, 2011.
- [14] N. Thakur, S. Devi and P. Upadhyay, "Grayscale image quality measure in spatial domain," in 2010 International Conference on Computer and Communication Technology (ICCCCT), Allahabad, Uttar Pradesh, India, 2010.
- [15] L. Zhang, L. Zhang, X. Mou and D. Zhang, "FSIM: A Feature Similarity Index for Image Quality Assessment," *IEEE Trans. on Image Process.*, vol. 20, p. 2378–2386, August 2011.
- [16] Xue, Wufeng, et al. "Gradient magnitude similarity deviation: A highly efficient perceptual image quality index." *IEEE transactions on image processing* 23.2 (2013): 684-695.
- [17] H. Z. Nafchi, A. Shahkolaei, R. Hedjam and M. Cheriet, "Mean Deviation Similarity Index: Efficient and Reliable Full-Reference Image Quality Evaluator," *IEEE Access*, vol. 4, p. 5579–5590, 2016.
- [18] L. Zhang and H. Li, "SR-SIM: A fast and high performance IQA index based on spectral residual," in 2012 19th IEEE International Conference on Image Processing, Orlando, 2012.
- [19] H. R. Sheikh and A. C. Bovik, "Image information and visual quality," *IEEE Trans. on Image Process.*, vol. 15, p. 430–444, February 2006.
- [20] L. Zhang, Y. Shen and H. Li, "VSI: A Visual Saliency-Induced Index for Perceptual Image Quality Assessment," *IEEE Trans. on Image Process.*, vol. 23, p. 4270–4281, October 2014.
- [21] J. Zhou, D. L. Civco and J. A. Silander, "A wavelet transform method to merge Landsat TM and SPOT panchromatic data," *International Journal of Remote Sensing*, vol. 19, p. 743–757, January 1998.
- [22] Z. Wang and A. C. Bovik, "A universal image quality index," *IEEE Signal Process. Lett.*, vol. 9, p. 81–84, March 2002.
- [23] Karu, Kalle, and Anil K. Jain. "Fingerprint classification." *Pattern recognition* 29.3 (1996): 389-404.
- [24] Nguyen, Dinh-Luan, Kai Cao, and Anil K. Jain. "Robust minutiae extractor: Integrating deep networks and fingerprint domain knowledge." 2018 International Conference on Biometrics (ICB). IEEE, 2018.
- [25] Terhørst, Philipp, et al. "MiDeCon: Unsupervised and Accurate Fingerprint and Minutia Quality Assessment based on Minutia Detection Confidence." 2021 IEEE International Joint Conference on Biometrics (IJCB). IEEE, 2021.
- [26] <https://www.nist.gov/services-resources/software/fingerprint-minutiae-viewer-fpmv>



10.22214/IJRASET



45.98



IMPACT FACTOR:
7.129



IMPACT FACTOR:
7.429



INTERNATIONAL JOURNAL FOR RESEARCH

IN APPLIED SCIENCE & ENGINEERING TECHNOLOGY

Call : 08813907089  (24*7 Support on Whatsapp)